



Article

# Grain Refinement Effect on the Hot-Tearing Resistance of Higher-Temperature Al–Cu–Mn–Zr Alloys

Adrian S. Sabau <sup>1,\*</sup> , Brian K. Milligan <sup>2</sup>, Seyed Mirmiran <sup>3</sup>, Christopher Glaspie <sup>3</sup>, Amit Shyam <sup>4</sup>, J. Allen Haynes <sup>4</sup>, Andres F. Rodriguez <sup>5</sup>, J.A. Gonzalez Villarreal <sup>5</sup>  and Jose Talamantes <sup>5</sup>

<sup>1</sup> Computational Sciences & Engineering Division, Oak Ridge National Laboratory, Oak Ridge, TN 37831, USA

<sup>2</sup> Metallurgical and Materials Engineering Department, Colorado School of Mines, Golden, CO 80401, USA; bmilliga@mines.edu

<sup>3</sup> Fiat Chrysler Automobiles North America, LLC., Auburn Hills, MI 48326, USA; seyed.mirmiran@fcagroup.com (S.M.); christopher.glaspie@fcagroup.com (C.G.)

<sup>4</sup> Materials Science and Technology Division, Oak Ridge National Laboratory, Oak Ridge, TN 37831, USA; shyama@ornl.gov (A.S.); haynesa@ornl.gov (J.A.H.)

<sup>5</sup> Nemak Monterrey, 66000 Garcia Monterrey, Mexico; Andres.Rodriguez@Nemak.com (A.F.R.); Alejandro.Gonzalez@nemak.com (J.A.G.V.); Jose.Talamantes@nemak.com (J.T.)

\* Correspondence: sabaua@ornl.gov; Tel.: +1-865-241-5145

Received: 9 March 2020; Accepted: 23 March 2020; Published: 25 March 2020



**Abstract:** The hot-tearing resistance of Al–Cu–Mn–Zr (ACMZ) alloys was investigated as a step toward introducing these new cast alloys for severe duty, higher-temperature applications, such as cylinder heads for down-sized, turbocharged automotive engines. Alloy Cu compositions were varied from 5 to 8 wt.%. Targeted Ti levels were 0.02, 0.1, and 0.2 wt.% via additions of the Al–5Ti–1B master alloy. Hot-tearing resistance was assessed by visual examination and ranking of the cracking severity in a multi-arm permanent mold casting. It was found that at high impurity contents (Fe and Si of 0.2 wt.% each), the Al–Cu–Mn–Zr alloy with 4.95 wt.% Cu exhibited the poorest hot-tearing resistance, irrespective of the grain refining amount. Microstructural analysis indicated an effective reduction in the grain size, as the Ti additions were increased to 0.02 and 0.1 wt.% Ti via the Al–Ti–B grain refiner. The finest grain size was attained with a 0.1 wt.% Ti. Based on the hot-tearing evaluation, it was found that the additional grain refining via the Al–5Ti–1B master alloy at 0.1 wt.% Ti significantly reduces the hot-tearing susceptibility at Cu contents greater than 7.3 wt.% for ACMZ alloys with low Fe and Si. These findings indicate that the best hot-tearing resistance was observed at a grain refiner level of 0.1 wt.% Ti and high Cu content (greater than 7.3 wt.%). This study indicates that these Al–Cu–Mn–Zr alloys, which possess excellent microstructural stability and mechanical properties at elevated temperatures, can also possess excellent hot-tearing resistance.

**Keywords:** casting; hot-tearing; aluminum; Al–Cu alloys

## 1. Introduction

Hot tearing is a major casting defect that is difficult to overcome, especially for multicomponent Al–Cu alloys, which are well known to be prone to hot tearing in semi-permanent mold castings used for automotive cylinder heads. The objective of this study was to investigate grain refinement effects on the hot-tearing resistance of a new family of cast Al–Cu alloys containing Mn and Zr additions. These alloys have been designed for microstructural stability and retention of mechanical properties at higher temperatures (>300 °C) and are referred to as Al–Cu–Mn–Zr (ACMZ) alloys [1].

Although a previous hot-tearing resistance study of several non-grain-refined ACMZ alloys indicated dramatic improvements in hot-tearing resistance due to Cu, at Cu additions of 7.3 and 8 wt.% [2], the hot-tearing resistance of ACMZ alloys still required further enhancement to enable casting of complex automotive components such as advanced cylinder heads, using common high-volume, commercial casting methods.

One of the key challenges for the high-volume production of automotive cast metal parts is the minimization of casting defects [2]. Hot tearing is one of the most detrimental solidification casting defects—the formation of which depends on both the local state of stress and interdendritic feeding of liquid due to the solidification shrinkage [3–5]. In general, hot-tearing resistance has been assessed based on the examination of cracking in castings after they are cooled to room temperature in regions where cross-sectional size changes by employing molds that provide geometrical constraints, in geometries that mimic features from production castings, such as ring [6], “dog-bone or I-beam” [7,8], or “finger-mold” [9,10] in sand molds [6,11–14] or permanent molds [15].

The ACMZ alloys that were considered in this study are strengthened via metastable  $\theta'$  precipitates, which are known to strengthen most Al-Cu and Al-Si-Cu alloys at temperatures below 200 °C [16]. Moreover, in ACMZ alloys, these metastable intermetallics ( $\text{Al}_2\text{Cu}$ ) can be stabilized to much higher temperatures by microalloying with additions of Mn and Zr, while also maintaining low Fe and Si levels, resulting in substantial improvements in mechanical properties at elevated temperatures as compared to other cast alloys [1,17,18]. For example, two variants of ACMZ alloys, with 5.0 wt.% Cu and 6.4 wt.% Cu, exhibited significant mechanical properties and microstructural stability after extended exposure (200 h) at temperatures up to 350 °C [1]. A higher copper level (~6.4 wt.% Cu) was found to increase alloy hardness over that of the alloy with 5.0 wt.% Cu, due to the increased volume fraction of the intermetallic strengthening precipitates. The effect of intermetallic grain boundary particles on tensile elongation was investigated for a series of ACMZ alloys with Cu contents varying between 6.0 and 9.0 wt.% [19]. Owing to their improved thermal stability, two ACMZ alloys were shown to exhibit superior creep resistance at 300 °C as compared to a conventional 206 Al-Cu alloy [20].

One approach to further improving hot-tearing resistance without detrimentally affecting the high-temperature stability of these ACMZ alloys is through grain refinement. For Al alloys, grain refinement has long been used to improve both mechanical properties and hot-tearing resistance [21]. Initially, grain refining via inoculation was introduced to improve the mechanical properties by the formation of a fine, uniform, and equiaxed grain structure [22,23]. For Al-Cu alloys, the hot-tearing resistance of castings with fine equiaxed dendritic morphologies were found to be greater than those with columnar dendritic morphologies [24,25]. However, the effect of grain refinement on hot tearing is not consistent for Al-Cu alloys. This inconsistency could be due to the wide range of process conditions, mold configurations, and alloy compositions (including minor additions) that lead to the formation of distinct intermetallics across various studies. For example, grain refining was found to not affect the hot tearing of the binary Al-Cu alloys, which were cast in sand molds with a superheat of 65 °C [14]. This is in contrast with the hot-tearing data of an Al-Cu system in graphite molds with a superheat of 250 °C [8]. For another Al-Cu system at 250 °C superheat [8], the hot-tearing-resistant composition was shifted from 7 wt.% (for the non-refined) to 5 wt.% (for the grain refined at 0.01 wt.% Ti addition). In general, for Al alloys, higher additions of grain refiner, e.g., 1 wt.% Ti for 7050 and 7010 Al alloys, were found to be detrimental to the hot-tearing resistance [26].

For commercial Al-Cu alloy 206, there are several studies that report a wide range of hot-tearing resistance with grain refinement. For example, hot tearing in a six-finger permanent mold of the Al alloy 206 (with 0.12 wt.% Fe and 0.06 wt.% Si) at 300 °C mold temperature was found not to be improved after grain refinement [9], whereas a reduction in hot tearing was observed after grain refinement of a modified 206 Al alloy (with 0.05 wt.% Fe and 0.05 wt.% Si) [27]. This difference could be simply due to the lower Fe content in the alloy used by Li et al. [27] or different pouring temperatures, which were not specified in that study [9]. This comparison illustrates that hot-tearing resistance does

not necessarily improve after grain refinement of Al–Cu alloys, and also suggests significant sensitivity to alloy composition including impurity levels.

The beneficial effect on hot tearing in Al alloys has been found to be due to the influence of grain refinement on several variables that affect interdendritic flow, particularly permeability and dendrite coherency [28]. Through grain refinement, the permeability of the mushy zone is likely to increase at high solid fractions as the dendritic morphology would allow an increased liquid amount per unit volume. For Al–Cu alloys, the onset of mushy zone strength was found to shift to higher solid fractions with grain refinement [29,30]. This effect was explained by the fact that dendrites are smaller, almost globular, and not as highly branched as those in the non-grain-refined alloys, allowing easier grain reorientation and sliding after the coherency point, moving the onset of strength at higher solid packing as solidification proceeds.

## 2. Alloy Selection and Grain Refining

In this study, ACMZ multicomponent alloys in which the Cu composition was varied from ~5 to 8 wt.% were considered since they exhibit excellent high-temperature mechanical properties [1]. A review of the Cu content effect on hot tearing in Al–Cu alloys indicated that data on hot-tearing susceptibility at Cu contents > 5 wt.% were much less common than that available for alloys with Cu contents < 5 wt.% [2]. The Cu contents of the five alloys (DA1, DA2, DA5, DA6, and DA7) in this study were 4.95, 6.2, 7.3, 8.3, and 8 wt.%, respectively. The composition of these alloys, which was considered for hot-tearing assessment using a smaller mold with load measurement capability [2], was slightly different than that shown in Table 1. Exact compositions of the five alloys evaluated in this study are shown in Table 1. For all the new ACMZ alloys considered, the nominal composition of the non-grain-refined condition included 0.06 wt.% Ti. Alloy DA6 had a similar nominal Cu content to that of alloy DA7 (Table 1), but intentionally higher Fe and Si. Our previous study of non-grain-refined ACMZ alloys found that those with higher Cu content (7.3 and 8 wt.% Cu, i.e., DA5 and DA7) were the most hot-tearing resistant [2]. Alloy 206 was chosen as a comparative baseline commercial alloy for this study as it is one of the multicomponent Al–Cu alloys used in automotive, aerospace, and other industries where lightweight castings with excellent mechanical performance are required [21].

**Table 1.** Nominal non-grain-refined alloy composition.

Alloy	Cu wt. [%]	Mn wt. [%]	Zr wt. [%]	Si wt. [%]	Fe wt. [%]	Mg wt. [%]	Ni wt. [%]
206	4.82	0.254	0.004	0.041	0.095	0.274	0.0065
DA1	4.95	0.106	0.147	0.051	0.1	0.0026	0.163
DA2	6.214	0.448	0.191	0.0587	0.0952		
DA5	7.316	0.441	0.168	0.0501	0.0983		
DA6	8.211	0.44	0.207	0.202	0.219		
DA7	8.01	0.451	0.187	0.0488	0.102		

The grain refining behavior of two 206 Al alloys was studied extensively by others [31]. Alloy A206, which is used in aerospace and other high-integrity applications, is a higher-purity version of the standard 206 Al alloy. Alloy B206 has similar purity requirements as A206 but its titanium level is limited to 0.1 wt.%, while the titanium level in the non-grain-refined A206 ranges from 0.15 to 0.25 wt.% [32]. According to a previous investigation [31], the alloy B206 was registered based on data on the effectiveness of the Al–Ti–B grain refining for alloy A206 when the overall level of Ti was less than 0.15 wt.% Ti [21].

The B206 alloys were grain refined elsewhere [33] using 0.01 and 0.02 wt.% Ti, following recommendations to limit the Ti content from Al–Ti–B grain refining to a maximum of 0.05 wt.% for the A206 [21]. A significant decrease in grain size was found for a minimum amount of 0.02 wt.% Ti that was added via the Al–Ti–B grain refiner for B206 [34]. The effect of grain refiners below the 0.05 wt.%

Ti limit on grain size of B206 was found [33] to be the same as that observed for B206 castings [34]. On the other hand, a minimum Ti content of 0.07 wt.% was used for the Al-4.5%Cu alloy elsewhere [35]. Apparently, the size of the equiaxed grains obtained with 0.01 wt.% or less of Ti [33] was approximately ten times larger than that observed for the binary Al-4.5%Cu alloy [35].

The most widely used inoculants for Al alloys are based on Al-Ti-B [36]. Al-5Ti-1B was used for the grain refinement in this study as it is one of the most common master alloys [37]. Based on the review on grain refining via the Al-5Ti-1B master alloy, the target Ti levels selected in this study were 0.02, 0.1, and 0.2 wt.%.

### 3. Casting Procedures and Microstructure Characterization

Multi-arm (MA) casting, which consists of six dog-bone arms of different lengths attached to a riser [9], was employed in this study for *e-situ* characterization of hot tearing (Figure 1). This MA casting approach was first used by Sigworth and DeHart [9], while four-arm casting was used in [10]. A picture of the casting prior to removal from the mold is shown in Figure 1a. The dimensions of each of the six arms are shown in Figure 1b.

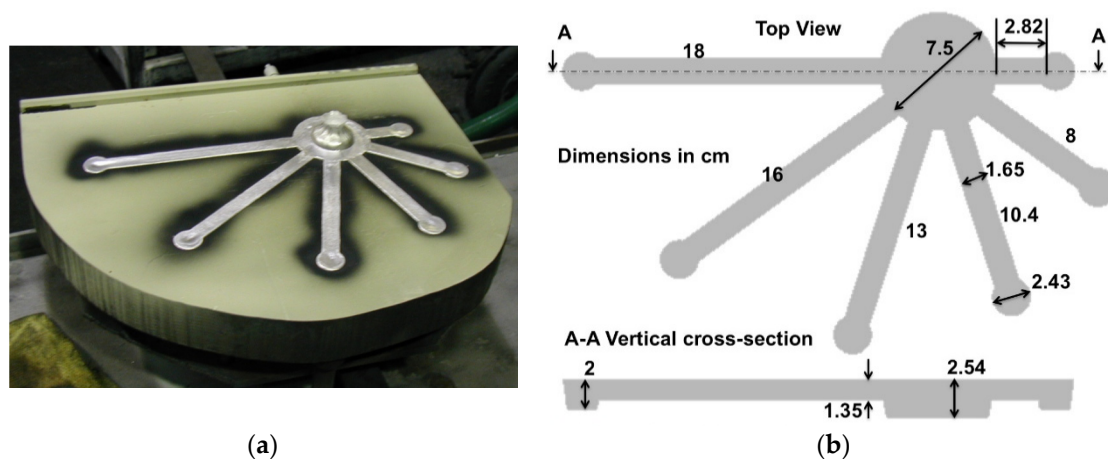


**Figure 1.** Multi-arm casting in permanent mold for hot-tearing assessment: (a) photo, and (b) geometry details and dimensions [cm].

The following casting procedure was followed at Nemak, Inc. For each casting run, approximately 270 kg of alloy was molten in a gas crucible furnace. The melt was heated to 770–780 °C and held at this temperature for ~30 min. For titanium and boron additions, a commercial Al-5Ti-1B master alloy rod was used. The target Ti contents were additional 0.02, 0.1, and 0.2 wt.% Ti via the master alloy. After degassing and dross removal from the melt, the grain refiner rod was added and allowed 20 min to melt. Meanwhile, the melt was gently stirred to ensure a uniform distribution of the grain refiner. Titanium and boron concentrations in the alloy were measured using optical emission spectroscopy. During the alloy melting, the mold was also prepared and preheated to the targeted temperature of 275 °C. The pouring temperature in this study was 730 °C. The casting was removed from the mold after two minutes. During this time, the mold heated to an average temperature of 315 °C. For each alloy, five castings were poured in the non-grain-refined condition and five castings for each grain-refined condition. In total, 115 multi-arm castings were poured and compared for this evaluation of hot-tearing resistance.

#### *Microstructure Characterization for the DA2 Alloy*

In this section, a detailed microstructure characterization is presented for the DA2 alloy in the as-aged condition, which consisted of solution annealing at 540 °C for 5 h and ageing at 240 °C for 4.5 h [1]. For all five ACMZ alloys considered, the grain size trends after inoculant additions varied in a similar way to that for the DA2 alloy and thus data for all alloys was not included in

this manuscript. Specimens from the various DA2 castings were cut from an arm centerline, ground, and polished. Grinding of specimens was conducted with wet SiC grinding papers, down to grit size 4000. Fine polishing was conducted with a MasterTex cloth (Buehler Inc., Lake Bluff, IL, USA) in a distilled water suspension with 50% Syton HT-50 colloidal silica, rinsing with water and ethyl alcohol. The grain structure was examined using a JEOL 6500 (JEOL Ltd., Tokyo, Japan) scanning electron microscope (SEM) employing electron backscatter diffraction (EBSD) in order to study grain sizes and orientations. The electron beam current was set to ~5 nA, and the incident-beam energy was set to 15 keV.

Typical SEM microstructures for all the conditions of the DA2 alloy are shown in Figure 2. The SEM micrographs indicate an effective reduction in grain size as the Ti additions were increased to 0.02 and 0.1 wt.% Ti via the Al-Ti-B grain refiner. The grain sizes and size distributions are revealed more clearly in the EBSD images of Figure 3. Grains with diameters of 30  $\mu\text{m}$  or less were not included in the EBSD analysis in order to filter out noise and eliminate the artifacts due to smaller intermetallic sizes. A further increase in the Ti addition to 0.2 wt.% Ti was found to slightly increase the grain size compared to the 0.1 wt.% Ti addition (Figures 2d and 3d). Quantitative analysis of the grain size was conducted using the SEM images. The grain size has been evaluated automatically using the EDAX OIM software (AMETEK, Inc., Berwyn, PA, USA) [38]. The surface area characterized was identical for all of the grain refinement levels. While almost 300 grains were counted for each of the grain-refined specimens, only approximately 30 grains were counted for the non-grain-refined specimen due to the much larger grain size. A histogram that describes grain size distribution is shown in Figure 4 for the non-grain-refined alloy and all of the grain-refined conditions. The overall grain size distribution for the non-grain-refined alloy, which is indicated in Figure 4a with a large dash line, exhibited a bimodal distribution. For the non-grain-refined DA2 alloy, the grain count indicates a similar number of very large grains (800–2000  $\mu\text{m}$ ) and fine grains (less than 80  $\mu\text{m}$ ), with only few medium size grains (200–300  $\mu\text{m}$ ). As qualitatively observed from the SEM and EBSD images, the grain size decreases with increasing Ti levels to 0.02 and 0.1 wt.%.

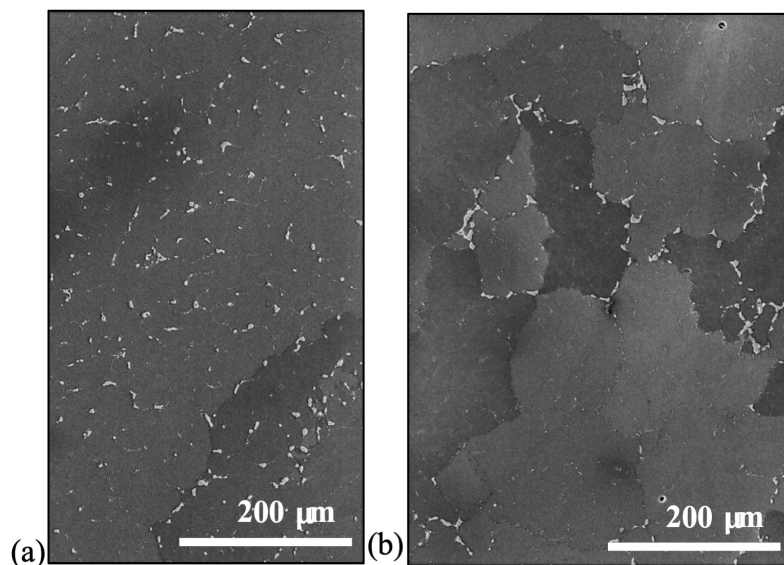
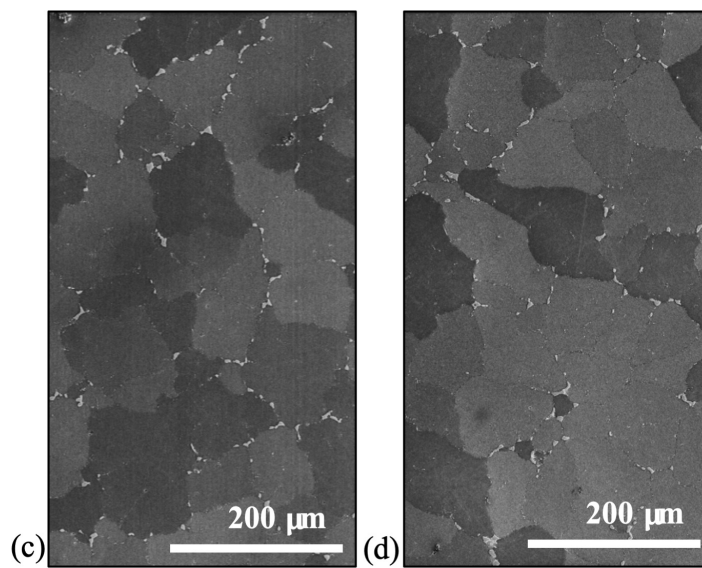
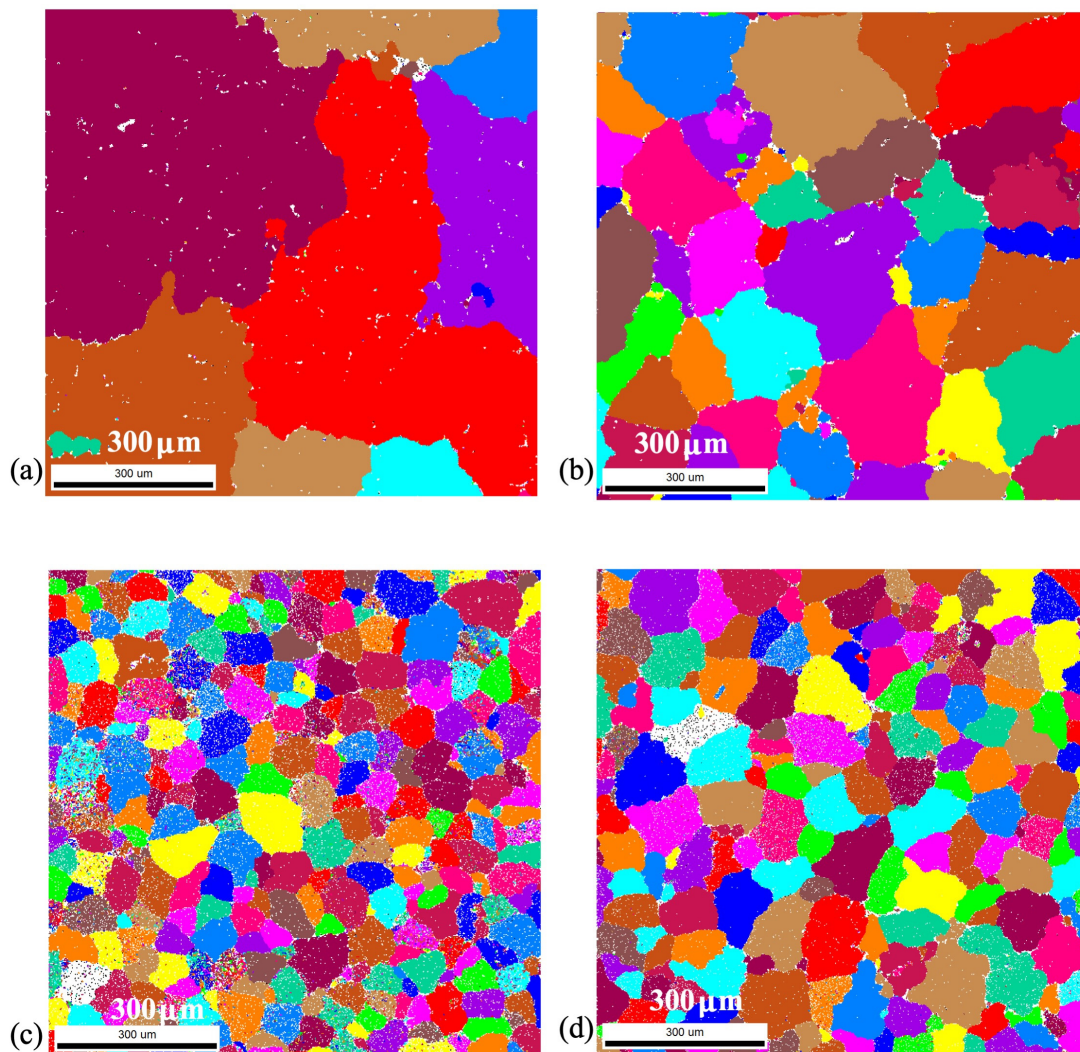


Figure 2. Cont.



**Figure 2.** Typical as-aged microstructure for the DA2 alloy for the (a) non-grain-refined condition and grain-refined conditions with (b) 0.02, (c) 0.1, and (d) 0.2 wt.% Ti.



**Figure 3.** Typical as-aged EBSD microstructure for the DA2 alloy for the (a) non-grain-refined condition and grain-refined conditions with (b) 0.02, (c) 0.1, and (d) 0.2 wt.% Ti.

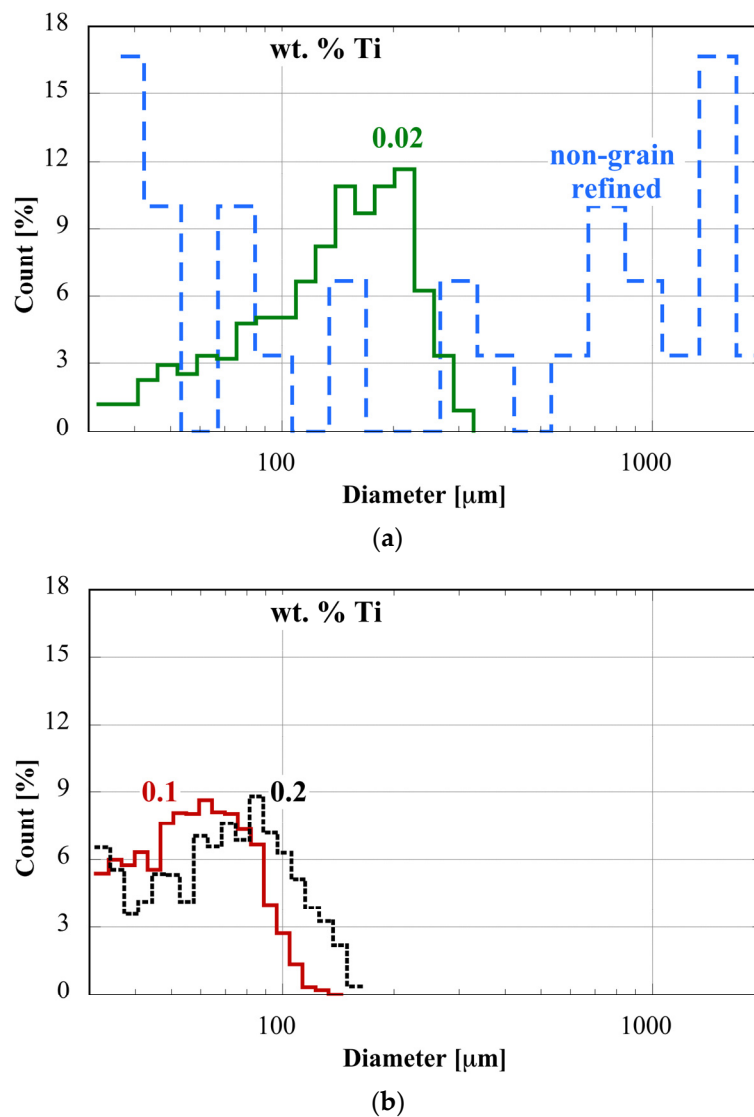


**Figure 4.** Grain size [μm] distribution for the DA2 alloy: (a) non-grain refined and grain refined with 0.02 wt.% Ti and (b) grain refined with 0.1 and 0.2 wt.% Ti (solid and dotted lines, respectively).

The SEM micrographs (Figure 2) reveal the variation in the morphology and density of the intermetallic particles, which appear in brighter contrast than the primary phases in the SEM micrographs. These particles are likely the primary eutectic  $\theta$  ( $Al_2Cu$ ) phase [39]. In the non-grain-refined alloy, these  $\theta$  particles appear both at the grain boundaries and on cellular boundaries within the grain bulk. However, in the grain-refined alloys, the  $\theta$  particles are concentrated only on the grain boundaries since the refined grain size is small enough that the cellular and grain boundaries coincide with each other. Several metrics for the intermetallic size and density characterization were included in Table 2. This data shows that despite the large difference in intermetallic particle distribution between the non-grain-refined specimen and the grain-refined specimens, there is only a weak dependence of the  $\theta$  particle size, number density, and phase fraction on the grain size.

**Table 2.** Median grain size [ $\mu\text{m}$ ] and parameters for intermetallic particle characterization for the DA2 alloy.

Ti wt.%	Median Grain Size ( $\mu\text{m}$ )	Intermetallic Area Fraction	Intermetallic Number Density ( $1/\mu\text{m}^2$ )	Intermetallic Average Area ( $\mu\text{m}^2$ )
0	525.6	0.0171	0.00141	12
0.02	137.2	0.0119	0.00094	13
0.1	57.8	0.0137	0.00087	18
0.2	70.1	0.0122	0.00098	12

The metastable  $\theta'$  (also  $\text{Al}_2\text{Cu}$ ) precipitate phase is also present. The  $\theta'$  phase is precipitated via solutionizing, water quench, and aging heat treatments [40]. After the ageing step at a temperature of 240 °C, it was shown in [1,16,19,20] that no Guinier–Preston (GP) zones, GP1, or GP2( $\theta''$ ) phases were stable and that the only strengthening phase that remains stable was the  $\theta'$  phase. During the solutionizing heat treatment, copper is dissolved into the matrix until the matrix composition is relatively homogeneous. The grain refiner content (and, by extension, the grain size) is unlikely to affect the size or distribution of the  $\theta'$  precipitates for the following reasons: (a) Cu content in all specimens were the same for all DA2 alloys with different grain refinement levels, (b) the composition was homogeneous after solutionizing, and (c)  $\theta'$  does not precipitate on grain boundaries. Thus, the only impact that grain size theoretically could have on  $\theta'$  precipitate distribution would be in the precipitate-free zone (PFZ), which is a region near the grain boundary that does not contain any precipitates [41]. For small grains, the PFZ would extend over a significant fraction of the microstructure, and the  $\theta'$  number density of the grain would be reduced. However, as the PFZ thickness was observed to be  $\sim 1 \mu\text{m}$  or less for these specimens in the as-aged condition, the PFZ covered a negligible fraction of the microstructure of the specimens tested here. Although not shown here, the SEM analysis for each of the specimens confirmed that the  $\theta'$  distributions and sizes appeared to be nearly identical for the grain-refined specimens considered.

#### 4. Hot-Tearing Characterization

During solidification, each arm in the MA casting experienced different stresses at the arm-riser junction due to the different geometrical constraints imposed by different arm lengths. Thus, the cracking severity is expected to be proportional to the arm length, i.e., smallest in shortest arms and largest in longest arms. All castings were visually inspected, and the severity of cracking in each arm was ranked according to the classification provided in Table 3. A simple scaling of hot-tearing resistance from the original cracking index range of [0:1], which was considered in [9], to a range of [0:10] was considered in this study in order to enable direct comparison with data presented in other papers using this mold. The cracking index was marked on each casting arm and a picture was taken for each casting of the riser region, where arms are joined to the riser and hot tearing is expected to occur. Due to the very large number of castings, images of only one representative casting for each alloy without any grain refining and at Ti additions of 0.02, 0.1, and 0.2 wt.% Ti were shown in Figures 5–8, respectively. In these figures, only the arm-riser joint region is shown in order to better indicate the hot-tearing defects in each arm. In Figures 5–8, pictures of the castings were taken after the castings were removed from the mold and turned upside down such that the shortest arm and longest arm appear to the left hand side and right hand side of each image, respectively.

Due to the severity of hot tearing for some alloys, the 6th arm was completely detached from the casting and is missing from pictures for DA1 and DA6 (Figure 5a,d for the non-grain-refined condition), DA1 (Figure 6a with 0.02 wt.% Ti), DA2 (Figure 7b with 0.1 wt.% Ti). For all of the alloys and for all grain refining conditions, there was no visible casting defect in the shortest arm.



Authors should discuss the results and how they can be interpreted in perspective of previous studies and of the working hypotheses. The findings and their implications should be discussed in the broadest context possible. Future research directions may also be highlighted.

**Table 3.** Assigned cracking index,  $C_i$ , for each casting arm.

$C_i$	Crack Description
0	No cracks
2.5	Small crack
5	Moderate crack
7.5	Severe crack
10	Arm fractured

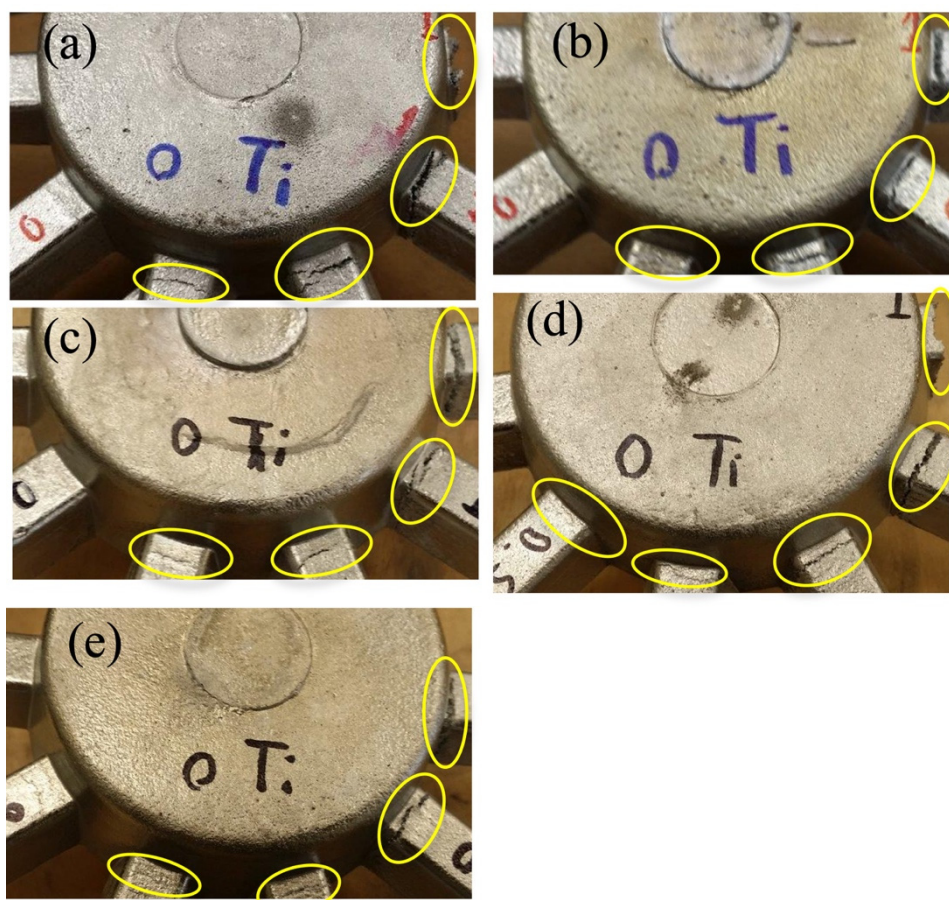


**Figure 5.** Pictures of representative multi-arm castings without grain refining: (a) DA1, (b) DA2, (c) DA5, (d) DA6, and (e) DA7.

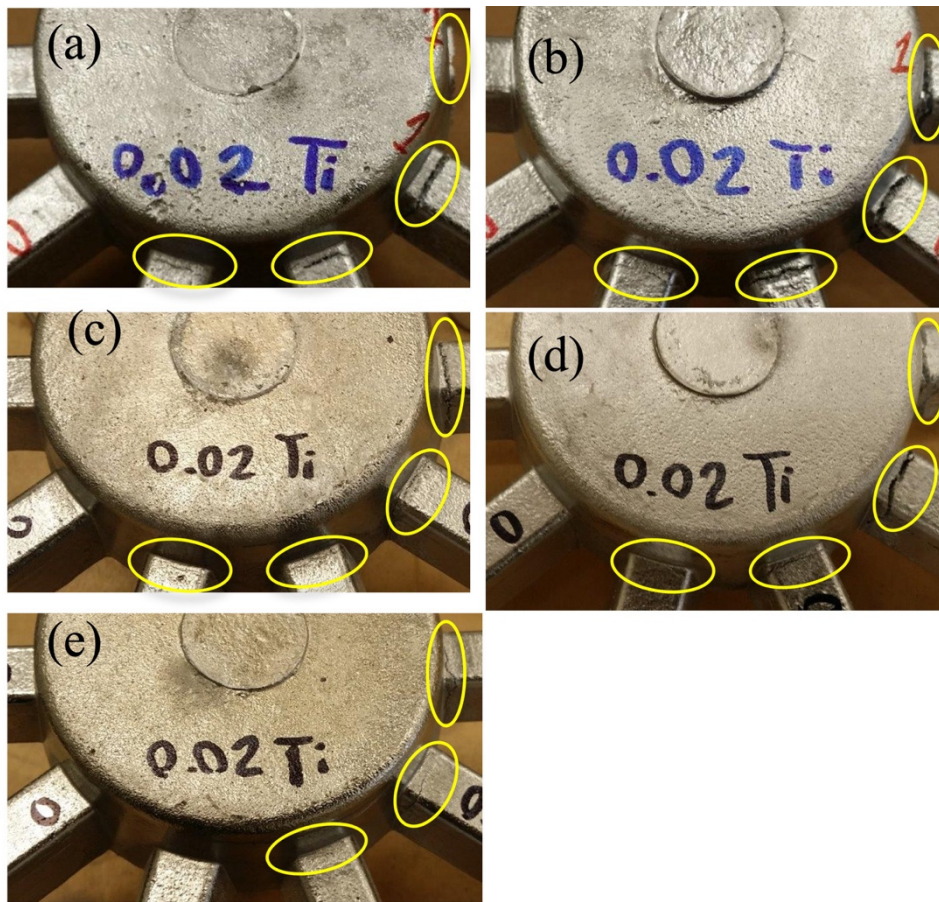


**Figure 6.** Pictures of representative multi-arm castings with 0.02 wt.% Ti addition: (a) DA1, (b) DA2, (c) DA5, (d) DA6, and (e) DA7.

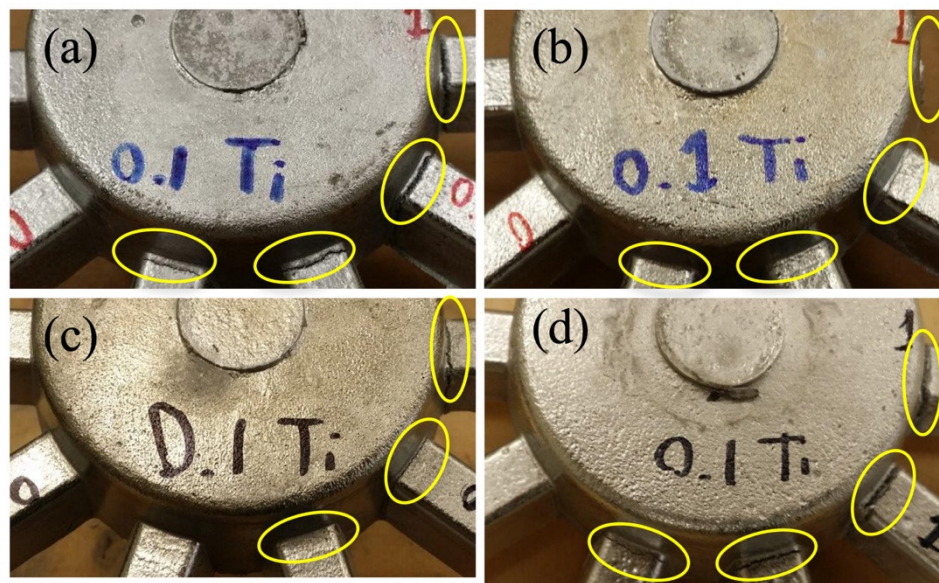


**Figure 7.** Cont.



**Figure 7.** Pictures of representative multi-arm castings with 0.1 wt.% Ti addition: (a) DA1, (b) DA2, (c) DA5, (d) DA6, and (e) DA7.

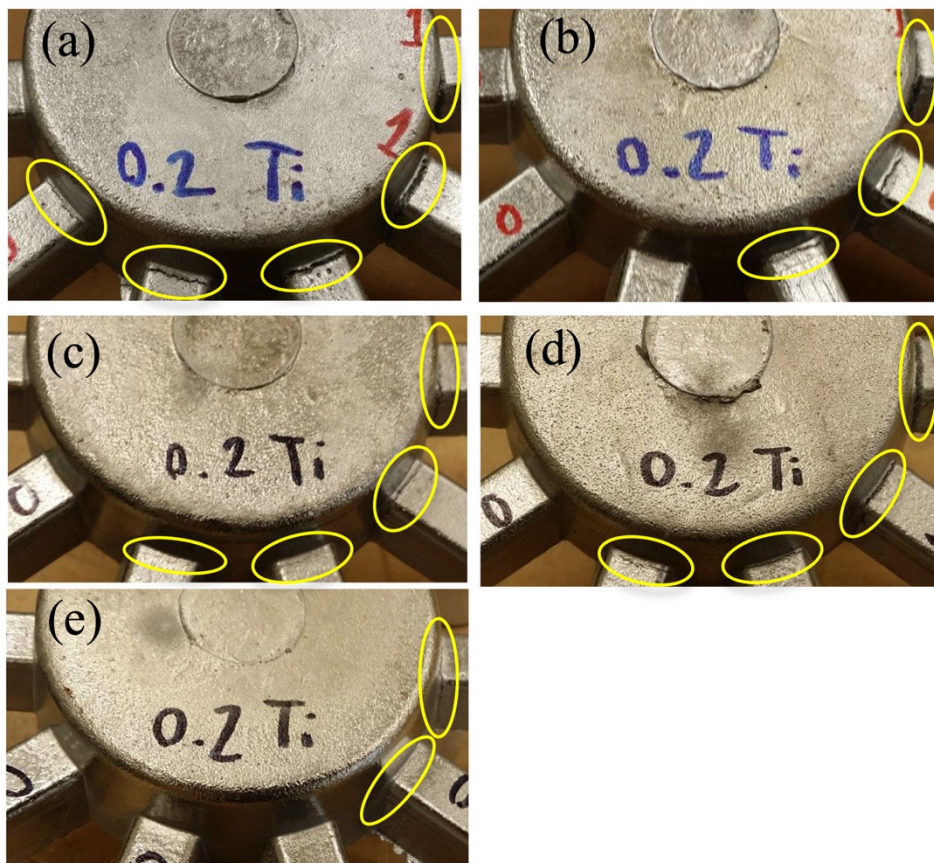


**Figure 8.** Pictures of representative multi-arm castings with 0.2 wt.% Ti addition: (a) DA1, (b) DA2, (c) DA5, (d) DA6, and (e) DA7.

Initially, the overall hot-tearing indicator (HTI) for this multi-arm casting was defined to be the simple average for all of the arms of individual cracking indices in each arm,  $C_i$ , as [9]:

$$M_S = \frac{1}{6} \sum_{i=1}^6 C_i \quad (1)$$

Several considerations have to be made concerning the use of individual cracking indices ( $C_i$ -Table 3) in each arm to formulate overall hot-tearing indices. In MA castings, cracks are likely to be more severe in longer arms than in shorter arms, thus identical cracking in different arms should yield different cracking susceptibilities, i.e., cracks in longer arms should have a smaller effect than those in shorter arms in the overall HTI. As the simple average indicator,  $M_S$ , does not take into account the higher probability of cracking in longer arms than in shorter arms, a weighted average of individual

cracking indices in each arm,  $C_i$ , was used. As it was observed that the shortest arm seldom cracks while the longest arm cracks most of the time, the effect of excluding the shortest arm (i.e., 1-st arm) and/or the longest arm (i.e., 6th arm) from the hot-tearing index needs to be considered. Thus, several hot-tearing indices can be defined based on cracking indices from several consecutive arms, as:

$$M_{J-K} = \frac{\sum_{i=J}^K w_i C_i}{\sum_{i=J}^K w_i} \quad (2)$$

where  $J$  and  $K$  indices indicate the shortest arm and longest arm that were considered in the weighted average, respectively. Here, the weight factor for each arm,  $i$ , was simply considered to be inversely proportional to the arm length,  $L_i$ , i.e.,  $w_i = \frac{1}{L_i}$  [33]. In the third and fourth columns of Table 4, the data is presented for the simple average indicator,  $M_S$ , and a 4-arm average,  $M_{2-5}$ , for which the arms 2 through 5 were considered, respectively. For the data shown in Table 4, the average of  $M_S$  and  $M_{2-5}$  for five castings were calculated based on Equations (1) and (2). From industrial practice, an overall acceptable hot-tearing index for  $M_S$ ,  $M_S^A$ , is considered to be 3.33 when  $C_i$  ranges between 0 and 10, which would correspond to a small to moderate crack in each of the six arms. Consistent with the acceptable value of  $M_S^A = 3.3$ , an overall acceptable hot-tearing index for  $M_{2-5}$ ,  $M_{2-5}^A$ , is considered to be 2.6 when  $C_i$  ranges between 0 and 10. The alloys and Ti concentration in wt.%, for which the acceptable hot-tearing resistance was attained, are: DA2 at 0.1 wt.% Ti, DA5 at 0.1 wt.% Ti, and DA7 at 0.02, 0.1, and 0.2 wt.% Ti. The data shown in Table 4 indicate that the  $M_S$  and  $M_{2-5}$  indices exhibit close values. The data shows that the  $M_{2-5}$  is larger than  $M_S$  for the least hot-tearing-resistant alloys (206 and DA6). On the other hand,  $M_{2-5}$  is smaller than  $M_S$  for the most hot-tearing-resistant alloys (DA5 and DA7).

The data shown in Table 4 on the hot-tearing indicator for multi-arm castings,  $M_{2-5}$ , indicate the following main effects of the grain refinement and Cu content on hot-tearing:

- For the 206 alloy,  $M$  exhibited a larger decrease from the non-grain-refined condition to that with 0.02 wt.% Ti additions than that from Ti additions of 0.02 to 0.1 wt.%.
- For the DA1 alloy,  $M$  increased slightly with grain refinement.
- For the DA2 alloy,  $M$  is initially unchanged with 0.02 wt.% Ti addition from the non-grain-refined casting. Then,  $M$  decreased with grain refinement with a minimum of HTI observed at 0.1 wt.% Ti addition.
- For the DA5 alloy,  $M$  decreased with grain refinement, exhibiting a minimum  $M$  at 0.1 wt.% Ti addition. Unlike DA1 and DA2,  $M$  showed a decrease between the non-grain-refined casting and the alloy with 0.02 wt.% Ti addition, a decrease that was similar in magnitude to that for the 206 alloy.
- For the DA6 alloy,  $M$  showed the highest value among all of the DA alloys considered. The  $M$  variation with the amount of wt.% Ti addition resembles that for DA1, although at high values. The striking difference between the  $M$  values for the DA5 and DA7 alloys is solely due to a higher amount of Fe and Si impurities in the DA6 alloy than those in the DA7 alloy.
- For DA7 alloy,  $M$  is the smallest among all of the DA alloys.  $M$  exhibited a *significant* decrease between the non-grain-refined casting and the alloy with 0.02 wt.% Ti addition.
- The minimum  $M$  is observed at 0.1 wt.% Ti addition for each of the most hot-tearing-resistant alloys (DA2, DA5, and DA7).

**Table 4.** Hot-tearing indices  $M_S$  and  $M_{2-5}$  from multi-arm castings.

Alloy (Cu wt.%)	* Ti wt.%	$M_S$	$M_{2-5}$
206 (4.82)	0	7.5	8.47
	0.02	6.67	7.07
	0.1	6.17	6.31
DA1 (4.95)	0	5.9	5.71
	0.02	6.25	6.4
	0.1	6.16	6.31
	0.2	6.25	6.4
DA2 (6.2)	0	5.4	5.1
	0.02	5.5	5.27
	0.1	3.42	2.6
	0.2	4.25	3.21
DA5 (7.3)	0	5.8	5.53
	0.02	4.25	4.03
	0.1	3.25	2.49
	0.2	3.42	2.84
DA6 (8.2)	0	6.5	6.71
	0.02	6.9	7.36
	0.1	6.6	6.88
	0.2	6.1	6.05
DA7 (8)	0	5.1	4.86
	0.02	3.33	2.6
	0.1	2.5	2.01
	0.2	2.75	2.36

\* Addition target (via the Al-Ti-B master alloy).

## 5. Discussions

To better clarify the effect of grain refining at different Cu contents on hot tearing, data shown in Table 4 is further analyzed. In Figure 9, the  $M_{2-5}$ , which was obtained as an average for arms 2 through 5, is graphed as a function target Ti addition wt.% at different Cu contents and low content of Fe and Si (of ~0.1 and 0.05 wt.%, respectively). For reference, the data on the baseline alloy 206 is also shown. The data shown in Figure 9 clearly indicates that grain refining of ACMZ alloys is much more effective at Cu contents greater than 7.3 wt.% (DA5 and DA7 alloys), with a minimum hot-tearing index value at 0.1 wt.% Ti additions, as evidenced by the significant reduction in the hot-tearing index.

The data for DA6, with higher Fe and Si impurity contents, is shown in Figure 10, along with the data from the corresponding low impurity alloy, DA7. Both of these alloys have a high nominal Cu content of ~8 wt.%. As shown in Figure 10, at high contents of Fe and Si (i.e., ~0.2 wt.% each), the hot-tearing index is high while the alloy with lower content of Fe and Si (~0.1 and 0.05 wt.%, respectively) shows significant reduction in hot-tearing index levels, and thus improvement in hot-tearing behavior, with grain refining and also some improvement in hot-tearing resistance with no grain refinement.

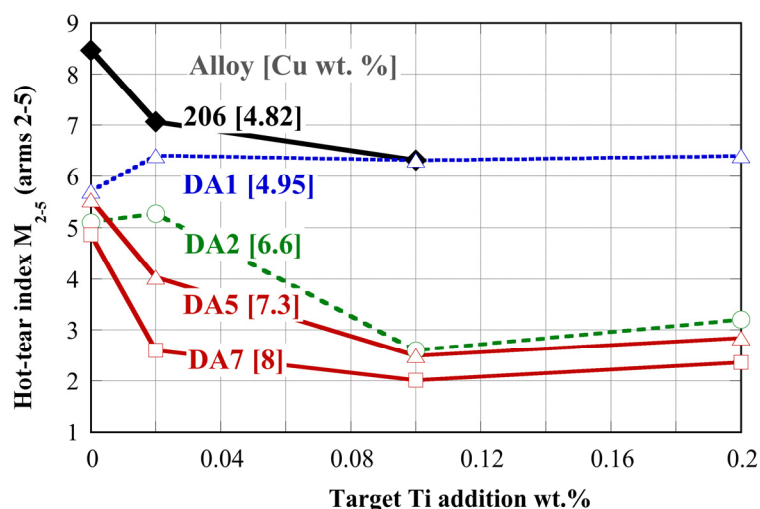


Figure 9. The hot-tearing index as a function of wt.% Ti addition for alloys 206, DA1, DA2, DA5, and DA7, all with low levels of Fe and Si impurities.

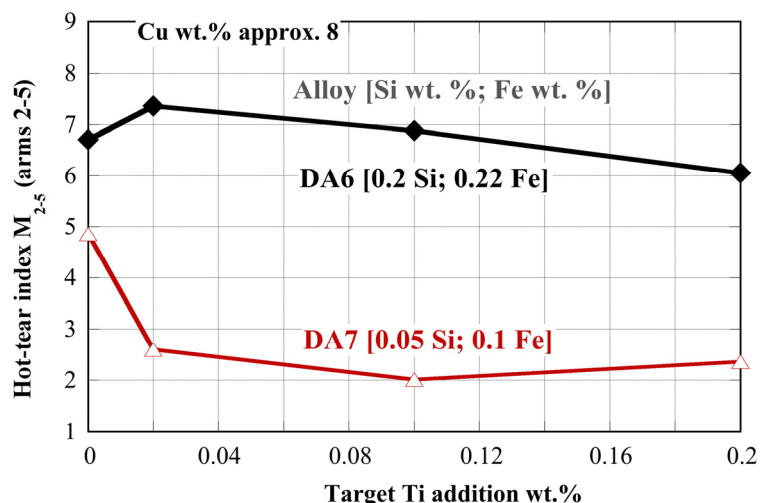


Figure 10. The HTI as a function of wt.% Ti addition for alloys DA6 and DA7 (Fe + Si effect).

Aside from the beneficial effect of the higher Cu content on hot-tearing resistance discussed above, the grain size effect is briefly discussed below for the DA2 alloy. The median grain size, which was obtained from the microstructure analysis is shown together with the hot-tearing index for all grain-refined conditions in Table 5. The data shows that at grain sizes larger than 130  $\mu\text{m}$ , the hot-tearing index exhibits insignificant variation with the reduction in grain size. However, at small grain sizes (less than 100  $\mu\text{m}$ ), the hot-tearing index decreases significantly with the smaller grain sizes.

Table 5. Hot-tearing indices  $M_5$  and  $M_{2-5}$  from multi-arm castings.

Alloy	Ti wt. %	Median Grain Size ( $\mu\text{m}$ )	$M_{2-5}$
DA2	0	525.6	5.1
	0.02	137.2	5.27
	0.1	57.8	2.6
	0.2	70.1	3.21

As reviewed in the previous sections, there is a wide range of hot-tearing resistance with grain refinement for alloys 206, A206, and B206. ASM specifications for wt.% Fe, Si, and Ti are 0.15, 0.1, 0.15–0.3 for 206, 0.1, 0.05, 0.15–0.3 for A206, and 0.1, 0.05, 0.10 for B206, respectively. Without being exhaustive, the recommended wt.% Ti grain refining for enhancing the mechanical properties and hot-tearing resistance is summarized in Table 6 for 206 alloys and the ACMZ alloys used in this study. It was found that the optimum wt.% Ti of 0.1 for ACMZ alloys is within the range recommended for the low-impurity and low-Ti 206 alloy [27] but larger than that recommended for the A206 and B206 alloys [9,33].

**Table 6.** Maximum and optimum Ti wt.% addition for hot-tearing resistance.

Alloy	wt.% Fe and wt.% Si	* wt.% Ti	Reference	Addition Max Ti wt.%	Notes
206	0.12 and 0.06	0.24	[9]	specified per ladle	grain refining not affecting hot tearing
206	0.05 and 0.05	0.006	[27]	0.15	optimum 0.1–0.15 wt.% Ti
A206	0.1 and 0.05	0.15–0.25	[9]	0.05	recommend $\leq 0.05$ wt.% Ti
B206	0.06 and 0.1	0.01	[33]	0.05	recommend [0.02:0.05] wt.% Ti range
ACMZ	0.07 and 0.08	0.06	This study	0.2	optimum 0.1 wt.% Ti

\* Nominal, non-grain-refined alloy composition.

## 6. Conclusions

The grain refinement effect on hot-tearing resistance for a new family of Mn- and Zr-containing Al-Cu alloys, termed ACMZ, was investigated using a six-arm casting, in which dog-bone arms of different lengths are attached to a riser. Alloy 206 was chosen as the baseline alloys for this study, as it is one of the multicomponent Al-Cu alloys used in several industries where high-mechanical-performance castings are needed. Based on a review of grain refining via the Al-5Ti-1B master alloy for Al-Cu alloys, and more specifically for alloy 206, the target Ti levels considered in this study were 0.02, 0.1, and 0.2 wt.%.

A detailed microstructure characterization is presented for the ACMZ alloy with 6.6 wt.% Cu in the as-aged condition. The overall grain size distribution for the non-grain-refined alloy, which included very large grains (800–2000  $\mu\text{m}$ ), exhibited a bimodal distribution. The SEM and EBSD micrographs indicate an effective reduction in the grain size as the Ti additions were increased to 0.02 and 0.1 wt.% Ti via the Al-Ti-B grain refiner. The finest grain size was attained with a 0.1 wt.% Ti. Despite the large difference in intermetallic distribution between the non-grain-refined specimen and the grain-refined specimens, there is only a weak dependence of the primary eutectic  $\theta$  ( $\text{Al}_2\text{Cu}$ ) phase particle size, number density, and phase fraction on the grain size. The metastable  $\theta'$  (also  $\text{Al}_2\text{Cu}$ ) precipitate phase appeared to be nearly identical for the grain-refined specimens considered.

All 115 castings were visually inspected, and the severity of cracking in each arm was ranked according to a [0:10] scale. The overall hot-tearing indicator was defined to be the weighted average,  $M_{J-K}$ , with the inverse of arm length, for individual cracking indices in several arms (J through K). The weighted average was considered a more appropriate metric for the hot-tearing index than the simple average, which it does not take into account the higher probability of cracking in longer arms than in shorter arms. Moreover, as the shortest arm seldom cracks, while the longest arm cracks most of the time,  $M_{2-5}$ , with the weighted average for cracking indices in arms 2 through 5 were considered. The least hot-tearing-resistant alloy was DA6 (8.2 wt.% Cu and high impurity contents of Fe and Si of  $\sim 0.2$  wt.% each) while the hot-tearing resistance of the DA7 alloy, with similar Cu content but lower impurity contents of Fe and Si of  $\sim 0.1$  and 0.05 wt.%, respectively, was the best. The overall hot-tearing indicator  $M_{2-5}$  indicated the following main effects of the grain refinement for alloys with low levels of Fe and Si impurities:

- Grain refining for the DA1 alloy (4.95 wt.% Cu) was ineffective, as  $M$  was slightly *higher* for all grain-refined conditions as compared to its non-refined condition.
- The hot-tearing resistance was highest for the DA7 alloy (with the highest Cu level at 8 wt.%), followed by the DA5 alloy (7.3 wt.% Cu). The hot-tearing resistance significantly increased with 0.02 wt.% Ti addition (from the non-grain-refined condition).
- The best hot-tearing resistance was observed at 0.1 wt.% Ti addition for the most hot-tearing-resistant alloys (DA2, DA5, and DA7). This finding is expected based on grain size analysis, as hot-tearing resistance increases with smaller grain size and the metallography observations indicate that the finest grain size was attained at 0.1 wt.% Ti.
- It was found that the optimum wt.% Ti of 0.1 for ACMZ alloys is within the range recommended for the low impurity and low Ti levels for the 206 alloy but larger than that recommended for the A206 and B206 alloys.

The assessment of the hot-tearing behavior as a function of composition and grain refining, in which a commercial-scale mold was used, is an important step for the introduction of ACMZ alloys for applications that demand very good high-temperature mechanical properties, such as modern automotive cylinder heads.

**Author Contributions:** Conceptualization: S.M., C.G. and A.S.; methodology: S.M., C.G., A.F.R., J.A.G.V. and J.T.; formal analysis: A.S.S., B.K.M. and A.F.R.; investigation: A.S.S., B.K.M., and A.F.R.; resources: J.A.G.V. and J.T.; data curation: A.S.S., B.K.M., and A.F.R.; writing—original draft preparation: A.S.S.; writing—review and editing: B.K.M., A.S., and J.A.H.; visualization: A.S.S.; supervision: A.S., and J.A.H.; project administration: A.S. and J.A.H.; funding acquisition: A.S. and J.A.H. All authors have read and agreed to the published version of the manuscript.

**Funding:** Research sponsored by the U. S. Department of Energy, Office of Energy Efficiency and Renewable Energy, Vehicle Technologies Office, as part of the Propulsion Materials Program under contract DE-AC05-00OR22725 with UT-Battelle, LLC.

**Acknowledgments:** This work was performed under a Cooperative Research and Development Agreement (CRADA) with Nemak Inc., and Fiat Chrysler Automobiles US LLC for the project "High Performance Cast Aluminum Alloys for Next Generation Passenger Vehicle Engines." Research sponsored by the U. S. Department of Energy, Office of Energy Efficiency and Renewable Energy, Vehicle Technologies Office, as part of the Propulsion Materials Program under contract DE-AC05-00OR22725 with UT-Battelle, LLC.

**Conflicts of Interest:** The authors declare no conflict of interest.

**Notice:** This manuscript has been authored in part by UT-Battelle, LLC, under contract DE-AC05-00OR22725 with the US Department of Energy (DOE). The United States Government retains and the publisher, by accepting the article for publication, acknowledges that the United States Government retains a non-exclusive, paid up, irrevocable, world-wide license to publish or reproduce the published form of this manuscript, or allow others to do so, for United States Government purposes. The Department of Energy will provide public access to these results of federally sponsored research in accordance with the DOE Public Access Plan (<http://energy.gov/downloads/doe-public-access-plan>).

## References

1. Shyam, A.; Roy, S.; Shin, D.; Poplawsky, J.D.; Allard, L.F.; Yamamoto, Y.; Morris, J.R.; Mazumder, B.; Idrobo, J.C.; Rodriguez, A.; et al. Elevated temperature microstructural stability in cast AlCuMnZr alloys through solute segregation. *Mater. Sci. Eng. A* **2019**, *765*, 138279. [[CrossRef](#)]
2. Sabau, A.S.; Mirmiran, S.; Glaspie, C.; Li, S.; Apelian, D.; Shyam, A.; Allen Haynes, J.; Rodriguez, A.F. Hot-Tearing Assessment of Multicomponent Nongrain-Refined Al-Cu Alloys for Permanent Mold Castings Based on Load Measurements in a Constrained Mold. *Metall. Mater. Trans. B* **2018**, *49*, 1267–1287. [[CrossRef](#)]
3. Campbell, J. *Castings*; Butterworth and Heineman, Ltd.: Oxford, UK, 1991.
4. Campbell, J.; Clyne, T. Hot tearing in Al-Cu alloys. *Cast Met.* **1990**, *3*, 224–226. [[CrossRef](#)]
5. Rappaz, M.; Drezet, J.M.; Gremaud, M. A new hot-tearing criterion. *Mater. Sci. Eng. A Sci.* **1999**, *30*, 449–455. [[CrossRef](#)]
6. Warrington, D.; McCartney, D. Development of a new hot-cracking test for aluminium alloys. *Cast Met.* **1989**, *2*, 134–143. [[CrossRef](#)]



7. Clyne, T.W. Solidification Cracking of Aluminium Alloys. Ph.D. Thesis, University of Cambridge, Cambridge, UK, 1976.
8. Spittle, J.; Cushway, A. Influences of superheat and grain structure on hot-tearing susceptibilities of Al-Cu alloy castings. *Met. Technol.* **1983**, *10*, 6–13. [[CrossRef](#)]
9. Sigworth, G.K.; DeHart, F. Recent developments in the high strength aluminum-copper casting alloy A206. *AFS Trans.* **2003**, *111*, 341–354.
10. Lin, S.; Aliravci, C.; Pekguleryuz, N.I.O. Hot-tear susceptibility of aluminum wrought alloys and the effect of grain refining. *Mater. Sci. Eng. A Sci.* **2007**, *38A*, 1056–1068. [[CrossRef](#)]
11. Rosenberg, R.A.; Flemings, M.C.; Taylor, H.F. Nonferrous Binary Alloys Hot Tearing. *AFS Trans.* **1960**, *58*, 518–528.
12. Davidson, C.; Viano, D.; Lu, L.; StJohn, D. Observation of crack initiation during hot tearing. *Int. J. Cast Met. Res.* **2006**, *19*, 59–65. [[CrossRef](#)]
13. Mathier, V.; Grasso, P.D.; Rappaz, M. A new tensile test for aluminum alloys in the mushy state: Experimental method and numerical modeling. *Mater. Sci. Eng. A Sci.* **2008**, *39A*, 1399–1409. [[CrossRef](#)]
14. Rosenberg, R.; Flemings, M.; Taylor, H. Nonferrous binary alloys hot tearing. *AFS Trans* **1960**, *69*, 518–528.
15. Li, S.; Sadayappan, K.; Apelian, D. Characterisation of hot tearing in Al cast alloys: Methodology and procedures. *Int. J. Cast Met. Res.* **2011**, *24*, 88–95. [[CrossRef](#)]
16. Shower, P.; Roy, S.; Hawkins, C.S.; Shyam, A. The effects of microstructural stability on the compressive response of two cast aluminum alloys up to 300 °C. *Mater. Sci. Eng. A* **2017**, *700*, 519–529. [[CrossRef](#)]
17. Shower, P.; Morris, J.; Shin, D.; Radhakrishnan, B.; Poplawsky, J.; Shyam, A. Mechanisms for stabilizing  $\theta'$ (Al<sub>2</sub>Cu) precipitates at elevated temperatures investigated with Phase Field modeling. *Materialia* **2019**, *6*, 100335. [[CrossRef](#)]
18. Shower, P.; Morris, J.R.; Shin, D.; Radhakrishnan, B.; Allard, L.F.; Shyam, A. Temperature-dependent stability of  $\theta'$ -Al<sub>2</sub>Cu precipitates investigated with phase field simulations and experiments. *Materialia* **2019**, *5*, 100185. [[CrossRef](#)]
19. Bahl, S.; Hu, X.; Hoar, E.; Cheng, J.; Haynes, J.A.; Shyam, A. Effect of copper content on the tensile elongation of Al–Cu–Mn–Zr alloys: Experiments and finite element simulations. *Mater. Sci. Eng. A* **2020**, *772*, 138801. [[CrossRef](#)]
20. Milligan, B.K.; Roy, S.; Hawkins, C.S.; Allard, L.F.; Shyam, A. Impact of microstructural stability on the creep behavior of cast Al–Cu alloys. *Mater. Sci. Eng. A* **2020**, *772*, 138697. [[CrossRef](#)]
21. Sigworth, G. Grain refining of aluminum casting alloys. In Proceedings of the Sixth International AFS Conference on Melt Treatment of Aluminum, Orlando, FL, USA, 11–13 November 2001; pp. 210–221.
22. Greer, A.L.; Cooper, P.S.; Meredith, M.W.; Schneider, W.; Schumacher, P.; Spittle, J.A.; Tronche, A. Grain refinement of aluminium alloys by inoculation. *Adv. Eng. Mater.* **2003**, *5*, 81–91. [[CrossRef](#)]
23. Greer, A. Grain refinement of alloys by inoculation of melts. *Philos. Trans. R. Soc. London, Ser. A* **2003**, *361*, 479–495. [[CrossRef](#)]
24. Pumphrey, W.I.; Lyons, J.V. Cracking during the casting and welding of the more common binary aluminium alloys. *J. Inst. Met.* **1948**, *74*, 439.
25. Easton, M.; Wang, H.; Grandfield, J.; St John, D.; Sweet, E. An analysis of the effect of grain refinement on the hot tearing of aluminium alloys. *Mater. Sci. Forum.* **2004**, *28*, 224–229.
26. Warrington, D.; McCartney, D. Hot-cracking in aluminium alloys 7050 and 7010-a comparative study. *Cast Met.* **1990**, *3*, 202–208. [[CrossRef](#)]
27. Li, S.; Sadayappan, K.; Apelian, D. Role of grain refinement in the hot tearing of cast Al-Cu alloy. *Metall. Mater. Trans. B* **2013**, *44*, 614–623. [[CrossRef](#)]
28. Spittle, J.A. Grain refinement in shape casting of aluminium alloys. *Int. J. Cast Met. Res.* **2006**, *19*, 210–222. [[CrossRef](#)]
29. Metz, S.A.; Flemings, M.C. Fundamental study of hot tearing. *Trans. Am. Foundrymen's Soc.* **1970**, *78*, 453.
30. Dahle, A.; Arnberg, L. Development of strength in solidifying aluminium alloys. *Acta Mater.* **1997**, *45*, 547–559. [[CrossRef](#)]
31. Fasoyinu, Y. *Energy Saving Melting and Revert Reduction Technology (Energy-SMARRT): Light Metals Permanent Mold Casting*; Technical Report for U.S. Department of Energy Office of Scientific and Technical Information: Oak Ridge, TN, USA, 2014. [[CrossRef](#)]

32. *Properties and Selection of Aluminum Alloys*; Kevin, A.; John, W.; Kaufman, J.G. (Eds.) ASM International: Geauga, OH, USA, 2019; Volume 2B. [[CrossRef](#)]
33. Kamga, H.K.; Larouche, D.; Bournane, M.; Rahem, A. Hot tearing of aluminum-copper B206 alloys with iron and silicon additions. *Mater. Sci. Eng. A* **2010**, *527*, 7413–7423. [[CrossRef](#)]
34. D'Elia, F.; Ravindran, C. 09-055 Effect of Ti-B Grain Refiner on Hot Tearing in Permanent Mold Cast B206 Aluminum Alloy. *Trans. Am. Foundrymen's Soc.* **2009**, *117*, 139.
35. Chadwick, H. Hot Shortness of Al 4.5% Cu Alloy. *Cast Met.* **1991**, *4*, 43–49. [[CrossRef](#)]
36. Sigworth, G.K.; Kuhn, T.A. Grain refinement of aluminum casting alloys. *Int. J. Metalcast.* **2007**, *1*, 31–40. [[CrossRef](#)]
37. Easton, M.; Qian, M.; Prasad, A.; StJohn, D. Recent advances in grain refinement of light metals and alloys. *Curr. Opin. Solid State Mater. Sci.* **2016**, *20*, 13–24. [[CrossRef](#)]
38. ASTM E-1382 T. *Standard Test Methods for Determining Average Grain Size Using Semiautomatic and Automatic Image Analysis*; ASTM International: Philadelphia, PA, USA, 1997; Volume 3.01, pp. 901–922.
39. Roy, S.; Allard, L.; Rodriguez, A.; Watkins, T.; Shyam, A. Comparative Evaluation of Cast Aluminum Alloys for Automotive Cylinder Heads: Part I-Microstructure Evolution. *Metall. Mater. Trans. A* **2017**, *48A*, 2529–2542. [[CrossRef](#)]
40. Porter, D.; Easterling, K. Precipitation in Age Hardening Alloys. In *Phase Transformations in Metals and Alloys*, 2nd ed.; Chapman and Hall: London, UK, 1992.
41. Unwin, P.N.T.; Lorimer, G.W.; Nicholson, R.B. The origin of the grain boundary precipitate free zone. *Acta Metall.* **1969**, *17*, 1363–1377. [[CrossRef](#)]



© 2020 by the authors. Licensee MDPI, Basel, Switzerland. This article is an open access article distributed under the terms and conditions of the Creative Commons Attribution (CC BY) license (<http://creativecommons.org/licenses/by/4.0/>).